

The tridentate metal-binding sites of the common glycoses†

Natascha Ghaschghaie, Thomas Hoffmann, Martin Steinborn and Peter Klüfers*

Received 3rd December 2009, Accepted 14th April 2010

First published as an Advance Article on the web 15th May 2010

DOI: 10.1039/b925537k

Co^{III}(tacn) and Ga^{III}(tacn) fragments (tacn = 1,4,7-triazacyclononane) are suitable metal probes for the detection of the tridentate chelating sites of a glycoses. Three moles of hydroxide per mole of cobalt or gallium support triple deprotonation of the chelating triol functions at a glycoses's backbone. The individual chelating sites are detected using 1D and 2D NMR techniques. The metal-binding sites always include the hydroxy function at the anomeric carbon atom. Chelators are derived from both the pyranose and the furanose isomers while forming five- and six-membered chelate rings by the use of *cis,cis*-1,2,3-triol functions. The assignment of less frequently occurring ligand isomers are supported by a DFT approach. Crystal-structure analysis on Na₄[Cr(β-D-Manf1,2,3H₋₃)₂]NO₃·8.5H₂O (Man = mannose) additionally upholds the NMR assignments.

Introduction

In the past few years, carbohydrates have increasingly found their way into coordination chemistry. Recent reviews have highlighted their contribution to a metal's ligand sphere, where they serve as the origin of chirality or biocompatibility. Normally, a carbohydrate backbone is equipped with metal-chelating functional groups such as nitrogen or phosphorus donors. At the same time, other functions are blocked, especially the reactive anomeric center.^{1–6} Unprotected carbohydrates, in contrast, seem to be unpopular with coordination chemists as direct metal chelators due to their “inherent multifunctionality” and “complicated stereochemistry”.⁷ From this skeptical viewpoint, trouble should ultimately be expected from the class of reducing sugars that come with an unprotected anomeric center. This particular reactive subclass of carbohydrates includes the parent monosaccharides (aldoses and ketoses = “glycoses”), the non-anomerically phosphorylated ketose phosphates, glycuronates, 2-amino-2-deoxyglycoses (“glycosamines”) and their *N*-acetylated derivatives, and the deoxy-glycoses. All these biochemically significant substances have, depending on one's viewpoint, a fascinating or disastrous property as potential ligands: they are configurationally unstable. In aqueous equilibria they develop a mixture of two furanose and two pyranose anomers as the major isomers, as well as small amounts of open-chain forms. Taken together with the multifunctionality of each isomer, the numerous potential metal-binding sites may result in chaotic coordination behaviour. In fact, numerous ligand isomers have been detected after the reaction of the common aldoses with a Pd^{II}N₂-type metal probe that detects the bidentate bonding mode of these ligands. However, there are rules as well as a suitable framework for their formulation: the ligand-library concept.⁸ Within this concept, a glycoses's configurational variability is interpreted as the ability to adapt the

chelating oxygen-atom pattern to the requirements of the metal's ligand-binding sites. Since the various configurations of a glycoses are interconvertible under the typical reaction conditions for metal chelation, a glycoses, though being a single pure substance, provides a metal with a dynamic library of various chelators of different characteristics.

The number of actually available library members strongly depends on their denticity. Whereas the above-mentioned bidentate library usually contains up to a dozen members, this number rapidly decreases for higher denticities. Examples include lyxose with a single isomer that is capable of tetradentate bonding (β-lyxofuranose), and mannose which provides only a single isomer that is able to coordinate as a pentadentate ligand (β-mannofuranose).^{9–11} The chance to observe a single ligand type in the case of a polydentate glycoses isomer, is clearly the reason that sound structural information, both in solution and the solid state, is available for these higher O_n patterns, since they form the only solution species. Tridentate glycoses chelation, which should be somewhere in-between in terms of complexity, has not been the subject of a general study until now. In this work, we report on tridentate metal chelation by the parent members of the reducing sugars, the glycoses themselves.

The metal probes used in this work are derived from octahedrally coordinated trivalent central metals which provide a *fac*-M^{III}N₃ fragment with a vacant triangular face: the C₃-symmetric Co^{III}(tacn) and the Ga^{III}(tacn) residue. Both of these form diamagnetic complexes that allow for the use of standard one- and two-dimensional NMR techniques. In addition, the chromium(III) centre without a spectator ligand was included in a preliminary part of the investigation.

Experimental

Methods and materials

Reagent-grade chemicals were purchased from Aldrich, Fluka, TCI Europe or Grüssing and used as supplied. All preparations were carried out under air atmosphere. An approximately 0.5 M

Department of Chemistry and Biochemistry of the Ludwig Maximilian University Munich, Butenandstr. 5-13, D-81377, Munich, Germany. E-mail: kluef@cup.uni-muenchen.de; Fax: +49 89 2180 77407

† Electronic supplementary information (ESI) available: Validation of DFT-assisted NMR assignment. CCDC reference number 756937. For ESI and crystallographic data in CIF or other electronic format see DOI: 10.1039/b925537k

erythrose solution was prepared by a procedure published by Perlin.¹²

NMR spectroscopy

NMR spectra were recorded at room temperature on a Jeol Eclipse 400 (¹H: 400 MHz, ¹³C{¹H}: 101 MHz) NMR spectrometer. The signals of the residual protons (¹H) in D₂O were used as an internal reference for the chemical shift in the ¹H NMR spectra. In order to obtain a reference signal in the ¹³C{¹H} NMR spectra, one drop of methanol was added to the sample tube (5 mm).¹³ Shift differences are given as $\delta(C_{\text{complex}}) - \delta(C_{\text{free sugar}})$. The values for the free sugars were taken from measurements of the sugar in neutral aqueous solution with one added drop of methanol to the sample tube as a reference signal in the ¹³C{¹H} NMR spectrum.

Species assignment

The ¹H and ¹³C{¹H} NMR signals were assigned by ¹H-¹H COSY45, DEPT135, ¹H-¹³C HMQC, and ¹H-¹³C HMBC experiments in D₂O. To assign the signal sets to individual species, results on ribofuranose 5-phosphate were chosen as the starting point.¹⁴ Subsequently, the close similarity of the individual shifts of structurally related species was used (Tables 1–4). The results were checked by using a modified Karplus relationship.¹⁵ Generally, the detection of a furanose form was facilitated by its characteristic C4 signal close to 80 ppm. To support the assignments made in the less frequent case of ¹C₄-D-pyranose chelation within the lyxose group, the shifts were predicted by a DFT-based procedure. The Gaussian 03 program package was used for the calculations.¹⁶ For gallium and cobalt, a CEP-4G effective core potential with the corresponding valence basis set was used (12 or 17 electrons in valence shell, respectively).¹⁷ Geometries were optimised by the BLYP method and 6-31+G(2d,p) basis sets for all atoms except gallium and cobalt. Stationary points were confirmed with subsequent frequency analyses. GIAO NMR chemical shifts were calculated by the PBE1PBE method and the same basis sets used in the geometry optimisation. Shifts refer to $\delta = 0$ for tetramethylsilane, calculated by the same procedure. In the NMR

Table 1 ¹³C NMR shifts of Ga^{III}(tacn)–glycofuranose complexes. $\Delta\delta$ is the difference of a shift in the presence of the metal probe and the free glycoside; $\Delta\delta$ is given if values for the free glycoside isomer are available. Bold-printed $\Delta\delta$ values indicate the metal-binding site. A star indicates that the enantiomer of the respective isomer is depicted in the schemes

Group	Aldose Ketose		C1 C2 C3 C4 C5 C6					
			C1	C2	C3	C4	C5	C6
	α -D-Eryf	δ	102.4	85.4	72.3	73.2		
		$\Delta\delta$	6.4	13.6	2.5	1.0		
α -D-Rib	α -D-Ribf	δ	103.1	84.9	75.1	85.6	62.8	
		$\Delta\delta$	6.2	13.4	4.5	2.0	0.9	
α -D-Rib	α -D-Allf	δ	102.8	84.9	74.2	85.8	72.5	63.6
α -D-Rib	β -D-Talf	δ	103.2	85.0	76.1	85.6	72.4	63.8
		$\Delta\delta$	6.1	13.8	4.5	2.6	1.0	0.4
α -D-Rib	α -D-Psif	δ	63.0	110.4	83.6	76.3	84.0	63.0
		$\Delta\delta$	-0.9	6.5	12.6	5.3	0.7	1.1
β -D-Lyx*	β -D-Lyxf	δ	103.7	78.9	75.3	86.0	63.6	
		$\Delta\delta$	7.7	5.7	3.2	5.2	1.9	
β -D-Lyx*	α -L-Gulf	δ	103.8	77.2	75.8	85.7	73.0	63.5
β -D-Lyx*	β -D-Manf	δ	103.6	78.2	74.5	86.0	73.2	63.7
β -D-Lyx*	β -D-Tagf	δ	63.8	110.9	77.9	76.9	85.0	63.1
		$\Delta\delta$	0.6	7.8	6.2	5.6	4.3	1.5

Table 2 ¹³C NMR shifts of Ga^{III}(tacn)–glycofuranose complexes. $\Delta\delta$ is the difference of a shift in the presence of the metal probe and the free glycoside; $\Delta\delta$ is given if values for the free glycoside isomer are available. Bold-printed $\Delta\delta$ values indicate the metal-binding site. The lyxose entry is based on the weak signals of a minor species with about 10% abundance with the Ga^{III}(Me₃tacn) probe; the line with the DFT label shows the calculated chemical shifts for the Ga^{III}(tacn) probe (see the DFT chapter for more information). The values for mannose refer to the Ga^{III}(Me₃tacn) probe as well. A star indicates that the enantiomer of the respective isomer is depicted in the schemes

Group	Aldose Ketose		C1 C2 C3 C4 C5 C6					
			C1	C2	C3	C4	C5	C6
α -D-Rib	α -D-Ribf	δ	101.0	73.4	74.3	86.9	63.2	
		$\Delta\delta$	4.1	1.9	3.7	3.3	1.3	
α -D-Rib	β -D-Talf	δ	100.9	73.4	75.3	86.8	72.9	63.6
		$\Delta\delta$	3.8	2.2	3.7	3.8	1.5	0.2
α -D-Rib	α -D-Psif	δ	63.4	107.3	71.3	75.4	85.4	63.4
		$\Delta\delta$	-0.5	3.4	0.3	4.4	2.1	1.5
β -D-Lyx*	β -D-Lyxf	δ	101.8	74.2	73.6	81.4	63.2	
		$\Delta\delta$	5.8	1.0	1.5	0.6	1.5	
β -D-Lyx*	β -D-Manf	δ	101.4	74.7	74.0	80.8	72.1	64.2

Table 3 ¹³C NMR shifts of Co^{III}(tacn)–glycopyranose complexes. $\Delta\delta$ is the difference of a shift in the presence of the metal probe and the free glycoside. Bold-printed $\Delta\delta$ values indicate the metal-binding site. The DFT line lists calculated chemical shifts. A star indicates that the enantiomer of the respective isomer is depicted in the schemes. The origin of the unexpected $\Delta\delta$ values for lyxose (different chair conformation of free and bonded ligand) is discussed in the text

Group	Aldose Ketose		C1 C2 C3 C4 C5 C6					
			C1	C2	C3	C4	C5	C6
β -D-Lyx*	β -D-Lyxp	δ	99.7	77.8	72.3	70.6	57.4	
		DFT δ	99.3	77.0	73.8	72.7	56.9	
		$\Delta\delta$	4.9	7.2	-1.0	3.5	-7.4	
β -D-Lyx*	α -L-Gulp	δ	100.0	77.8	73.5	70.7	64.7	62.2
		$\Delta\delta$	6.6	12.6	2.0	0.7	-2.3	0.6
β -D-Lyx*	β -D-Tagp	δ	66.2	104.1	76.9	73.2	70.9	59.0
		$\Delta\delta$	2.1	5.2	12.6	2.8	1.0	-1.7

Table 4 Observed and calculated ¹³C NMR shifts of Ga^{III}(tacn)–glycopyranose complexes. $\Delta\delta$ is the difference of a shift in the presence of the metal probe and the free glycoside. Bold-printed $\Delta\delta$ values indicate the metal-binding site. The DFT line lists calculated chemical shifts. A star indicates that the enantiomer of the respective isomer is depicted in the schemes. The origin of the unexpected $\Delta\delta$ values for lyxose (different chair conformation of free and bonded ligand) is discussed in the text

Group	Aldose Ketose		C1 C2 C3 C4 C5 C6					
			C1	C2	C3	C4	C5	C6
β -D-Lyx*	β -D-Lyxp	δ	97.8	65.5	72.5	71.6	57.7	
		DFT δ	97.0	65.8	72.8	71.2	56.2	
		$\Delta\delta$	3.0	-5.1	-0.8	4.5	-7.1	
β -D-Lyx*	α -L-Gulp	δ	97.5	65.5	73.2	70.9	64.7	62.2
		$\Delta\delta$	4.1	0.3	1.8	0.9	-2.3	0.6
β -D-Lyx*	β -D-Tagp	δ	66.3	101.0	64.0	72.8	71.1	58.8
		$\Delta\delta$	2.2	2.1	-0.3	2.4	1.2	-1.9

calculations, a PCM model was used to simulate the influence of the solvent. The resulting chemical shifts were corrected using a linear relationship between the calculated and observed shift values (Fig. S1, ESI†). In the NMR-related Tables 1 to 4, the “coordination-induced shift” (CIS), the difference of the ¹³C NMR chemical shift of the metal-bonded and the free glycoside, is reported if the values for the free glycoside were available.

Synthesis and ^1H NMR data

Cobalt(III) complexes. To a solution of cobalt(II) chloride hexahydrate (0.048 g, 0.2 mmol) in D_2O (2.0 mL), 1,4,7-triazacyclononane trihydrochloride (0.048 g, 0.2 mmol), erythrose solution (0.3 mL, 0.2 mmol) or the respective pentose (0.030 g, 0.2 mmol) or hexose (0.036 g, 0.2 mmol) and sodium hydroxide (0.048 g, 1.2 mmol) were added under continuous stirring at room temperature. Alternatively, 1,4,7-triazacyclononane (0.026 g, 0.2 mmol) was used, in which case half of the sodium hydroxide (0.024 g, 0.6 mmol) was added. After the addition of 0.2 g active charcoal, the mixtures were heated to 50 °C for 2 h under vigorous stirring. Clear pink-red solutions were obtained after filtration and centrifugation.

^1H NMR (399.8 MHz, D_2O): ribose: $\delta = 4.48$ (d, 1H, $^3J_{\text{H}_1,\text{H}_2} = 3.30$ Hz, H1), 3.95–3.92 (m, 1H, H4), 3.75–3.73 (m, 1H, H2), 3.55–3.47 (m, 2H, H5/H5'), 3.17 (d, 1H, $^3J_{\text{H}_3,\text{H}_2} = 4.12$ Hz, H3), tacn: 3.32–3.27 (m), 3.14–2.93 (m), 2.81–2.60 (m). Lyxose: ^1H NMR (399.8 MHz, D_2O): $\delta = 4.71$ (d, 1H, $^3J_{\text{H}_1,\text{H}_2} = 3.30$ Hz, H1-*p*), 4.42 (d, 1H, $^3J_{\text{H}_1,\text{H}_2} = 3.57$ Hz, H1-*f*), 4.25–4.22 (m, 1H, H5-*p*), 3.90–3.89 (m, 1H, H4-*p*), 3.87–3.86 (m, 2H, H5-*f*/H5'-*f*), 3.77–3.75 (m, 1H, H4-*f*), 3.53–3.50 (m, 1H, H2-*f*), 3.47–3.45 (m, 1H, H3-*f*), 3.44–3.39 (m, 2H, H3-*p*/H2-*p*), 3.26–3.23 (m, 1H, H5'-*p*), tacn: 3.19–2.94 (m), 2.83–2.59 (m). Allose: ^1H NMR (399.8 MHz, D_2O): $\delta = 4.48$ (d, 1H, $^3J_{\text{H}_1,\text{H}_2} = 3.30$ Hz, H1), 3.83–3.81 (m, 1H, H4), 3.75–3.73 (m, 1H, H2), 3.71–3.69 (m, 1H, H6), 3.59–3.56 (m, 1H, H5), 3.54–3.53 (m, 1H, H6'), 3.28 (d, 1H, $^3J_{\text{H}_3,\text{H}_2} = 4.12$ Hz, H3), tacn: 3.35–3.29 (m), 3.17–2.92 (m), 2.82–2.60 (m). Mannose: ^1H NMR (399.8 MHz, D_2O): $\delta = 4.48$ (d, 1H, $^3J_{\text{H}_1,\text{H}_2} = 3.30$ Hz, H1), 4.06–4.02 (m, 1H, H5), 3.84–3.81 (m, 2H, H4/H6), 3.70–3.66 (m, 1H, H6'), 3.58–3.56 (m, 1H, H3), 3.51–3.49 (m, 1H, H2), tacn: 3.37–3.30 (m), 3.24–2.98 (m), 2.89–2.68 (m). Gulose: ^1H NMR (399.8 MHz, D_2O): $\delta = 4.47$ (d, 1H, $^3J_{\text{H}_1,\text{H}_2} = 3.30$ Hz, H1-*f*), 4.39 (d, 1H, $^3J_{\text{H}_1,\text{H}_2} = 3.57$ Hz, H1-*p*), 4.34–4.31 (m, 1H, H5-*p*), 4.13–4.10 (m, 1H, H5-*f*), 3.92–3.91 (m, 1H, H4-*p*), 3.79–3.77 (m, 1H, H4-*f*), 3.72–3.62 (m, 4H, H6-*f*/H6'-*f*/H6-*p*/H6'-*p*), 3.52–3.49 (m, 2H, H3-*f*/H2-*f*), 3.47–3.45 (m, 2H, H2-*p*/H3-*p*), tacn: 3.35–3.26 (m), 3.21–2.94 (m), 2.86–2.61 (m). Talose: ^1H NMR (399.8 MHz, D_2O): $\delta = 4.50$ (d, 1H, $^3J_{\text{H}_1,\text{H}_2} = 3.30$ Hz, H1), 3.89–3.88 (m, 1H, H4), 3.77–3.75 (m, 1H, H2), 3.72–3.60 (m, 2H, H5/H6), 3.55–3.50 (m, 1H, H6'), 3.21 (d, 1H, $^3J_{\text{H}_3,\text{H}_2} = 4.12$ Hz, H3), tacn: 3.34–3.26 (m), 3.18–2.93 (m), 2.83–2.61 (m).

Gallium(III) complexes. To a solution of gallium(III) chloride (0.021 g, 0.12 mmol) in D_2O (1.2 mL), 1,4,7-triazacyclononane trihydrochloride (0.029 g, 0.12 mmol), D-ribose (0.018 g, 0.12 mmol) or D-tagatose, L-gulose, D-talose or D-psicose (0.022 g, 0.12 mmol) and sodium hydroxide (0.029 g, 0.72 mmol) were added under continuous stirring at room temperature. The colourless mixtures were stirred for 15 min at room temperature. Variation for lyxose and mannose: gallium chloride (0.029 g, 0.16 mmol), D_2O (1.6 mL), *N,N',N''*-trimethyl-1,4,7-triazacyclononane (0.027 g, 0.16 mmol, 0.030 mL), D-lyxose (0.024 g, 0.16 mmol) or D-mannose (0.029 g, 0.16 mmol), sodium hydroxide (0.026 g, 0.64 mmol).

^1H NMR (399.8 MHz, D_2O): ribose: $\delta = 5.26$ (d, 1H, $^3J_{\text{H}_1,\text{H}_2} = 3.85$ Hz, H1), 4.16 (t, 1H, $^3J_{\text{H}_4,\text{H}_5} = 4.67$ Hz, H4), 4.13 (dd, 1H, $^3J_{\text{H}_2,\text{H}_1} = 3.85$ Hz, $^3J_{\text{H}_2,\text{H}_3} = 4.95$ Hz, H2), 3.82 (d, 1H, $^3J_{\text{H}_3,\text{H}_2} = 4.95$ Hz, H3), 3.65–3.56 (m, 2H, H5/H5'), tacn: 3.29–3.12 (m), 2.90–2.82 (m). Lyxose: $\delta = 5.08$ (d, 1H, $^3J_{\text{H}_1,\text{H}_2} = 3.02$ Hz, H1),

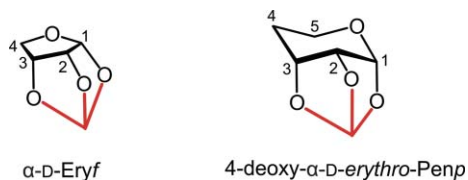
4.35 (m, 1H, H5), 3.89 (d, 1H, $^3J_{\text{H}_4,\text{H}_3} = 3.85$ Hz, H4), 3.72–3.70 (m, 1H, H3), 3.61 (m, 1H, H2), 3.35 (m, 1H, H5'), Me₃tacn: 3.06–2.85 (m), 2.81–2.63 (m), 2.46–2.36 (m). Gulose: $\delta = 5.10$ (d, 1H, $^3J_{\text{H}_1,\text{H}_2} = 3.02$ Hz, H1), 4.35–4.32 (m, 1H, H5), 3.89 (d, 1H, $^3J_{\text{H}_4,\text{H}_3} = 3.85$ Hz, H4), 3.77–3.71 (m, 4H, H6/H6'/H3/H2), tacn: 3.27–3.15 (m), 2.91–2.83 (m). Talose: $\delta = 5.22$ (d, 1H, $^3J_{\text{H}_1,\text{H}_2} = 3.57$ Hz, H1), 4.14–4.12 (m, 2H, H2/H4), 3.92–3.78 (m, 4H, H6/H6'/H3/H5), tacn: 3.28–3.10 (m), 2.90–2.81 (m).

Crystal-structure analysis†

A green crystal of the homoleptic bis(mannosato)chromate $\text{Na}_4[\text{Cr}(\beta\text{-D-Manf}1,2,3\text{H}_{-3})_2]\text{NO}_3 \cdot 8.5\text{H}_2\text{O}$ was selected with the aid of a polarisation microscope, mounted on the tip of a glass fibre and investigated at room temperature on a Nonius KappaCCD diffractometer with graphite-monochromated Mo-K α radiation ($\lambda = 0.71073$ Å). The structure was solved by direct methods (SIR 97) and refined by full-matrix least-squares calculations on F^2 (SHELXL-97).^{18,19} Anisotropic displacement parameters were refined for all non-hydrogen atoms. Further details: $\text{C}_{12}\text{H}_{35}\text{CrNNa}_4\text{O}_{23.5}$, $M_r = 713.35$ g mol⁻¹, $0.15 \times 0.12 \times 0.08$ mm, monoclinic, $P2_1$, $a = 8.3571(1)$, $b = 17.7714(3)$, $c = 9.2378(2)$ Å, $\beta = 96.1433(9)^\circ$, $V = 1364.09(4)$ Å³, $Z = 2$, $\rho = 1.7368(1)$ g cm⁻³, $T = 293(2)$ K, $\mu(\text{Mo-K}\alpha) = 0.587$ mm⁻¹, no absorption correction, θ range: 3.48–27.49°, 19477 refls., 6132 independent and used in refinement, 5709 with $I \geq 2\sigma(I)$, $R_{\text{int}} = 0.0317$, mean $\sigma(I)/I = 0.0476$; H atom refinement: C-bonded H: AFIX riding with $U(\text{H}) = 1.2 U(\text{C})$ for CH₂ and CHO-bonded H: AFIX 83 riding with $U(\text{H}) = 1.5 U(\text{O})$; 314 parameters, $R(F_{\text{obs}}) = 0.0477$, $R_w(F^2) = 0.1268$, $S = 1.023$, Flack parameter: $-0.01(2)$, min. and max. residual electron density: $-0.728, 0.956$ e Å⁻³, max. shift/error: 0.001. Note that the atomic numbering was altered for Fig. 3. Xn transforms to $Xn1$ and Xn' to $Xn2$ in the CIF (X = C, O).

Results and discussion

Tridentate chelation is connected with a restricted number of library members compared to bidentate chelation. Taking into account the formation of five- and six-membered chelate rings, the requirement of three oxygen donors in a *cis-cis* sequence leads to a few fundamental bonding types: furanose- $\kappa\text{O}^{1,2,3}$ for an aldotetrose, plus furanose- $\kappa\text{O}^{2,3,5}$, pyranose- $\kappa\text{O}^{1,2,3}$, and pyranose- $\kappa\text{O}^{2,3,4}$ for an aldopentose, plus further patterns for hexoses. In this study, we gained spectroscopic evidence for those two types of ligands that (1) include the anomeric centre in metal bonding, and (2) contribute exclusively oxygen donors bonded to a ring-carbon atom. Accordingly, the complexes of this work were found to match either the furanose- and/or the pyranose- $\kappa\text{O}^{1,2,3}$ pattern ($\kappa\text{O}^{2,3,4}$ for a ketose). The basic tridentate patterns thus are provided by α -D-erythrofurano (Scheme 1, left) and by the $^4\text{C}_1$ -conformer of 4-deoxy- α -D-erythro-pentopyranose (Scheme 1, right). The actual ligands of this work are derived from these parent chelating patterns by the addition of the specific functional groups of the individual glycoses. (To make visible the relationship of a glycoside to its respective basic tridentate pattern, the schemes show the required enantiomer even in those cases where the actual experiment was run with the other enantiomer. Since no chiral



Scheme 1 The spectroscopically observed O_3 patterns provided by the glycoses of this work. By adding a hydroxymethyl function to the 4-position *anti* or *syn* to the O_3 set, α -D-erythrofuranose (left) branches to α -D-ribofuranose (Scheme 2) and β -L-lyxofuranose (Scheme 3), respectively. By adding a 4-hydroxy function *syn* or *anti* to the O_3 set, 4-deoxy- α -D-erythro-pentopyranose (right) branches to α -D-ribo- and β -L-lyxopyranose, respectively.

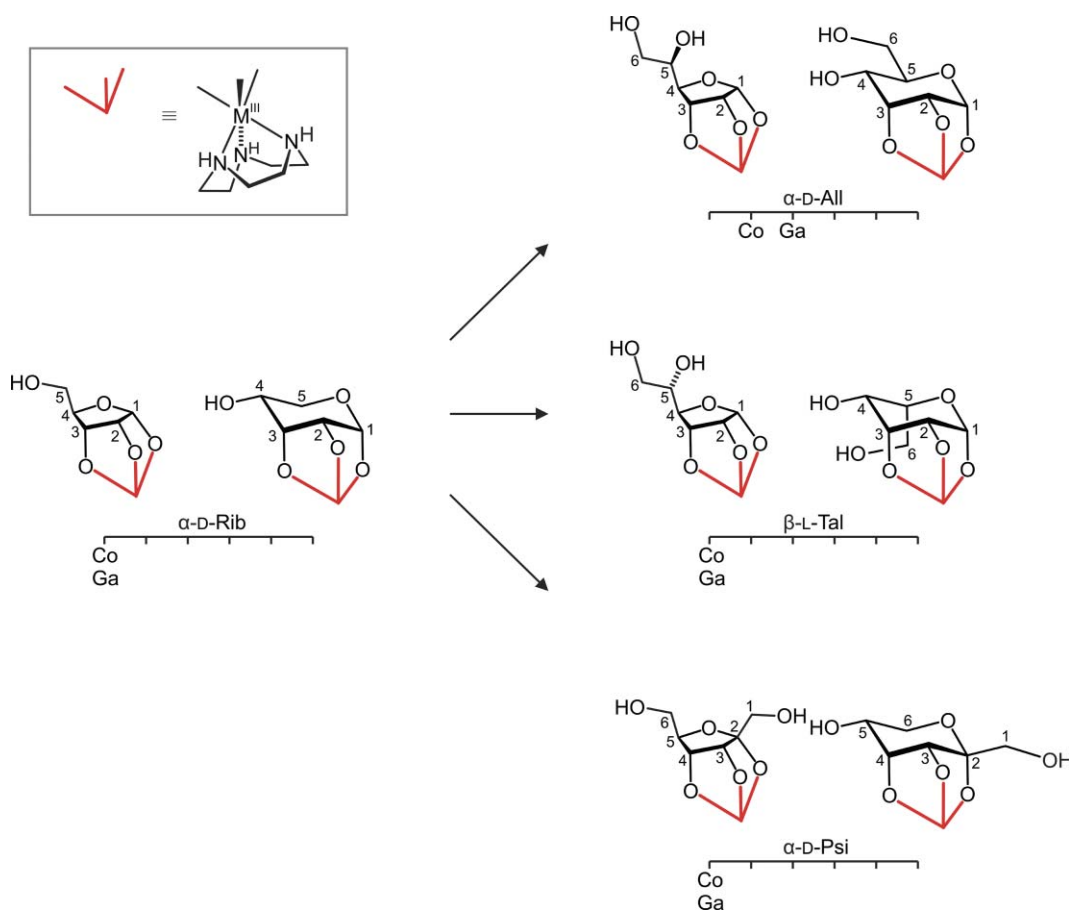
spectator ligands were used in this work, the relevant spectroscopic data remain the same.)

Using this approach, only half of the glycoses appear as potential tridentate chelators since threofuranose and its aldopentose (arabinose and xylose) and aldohexose (altrose, galactose, glucose, idose) homologues are not capable of providing a tridentate ligand by their furanose moiety to a single metal centre due to the *trans* configuration of at least two hydroxy functions. Accordingly, the schemes contain one half each of the two aldotetroses, four

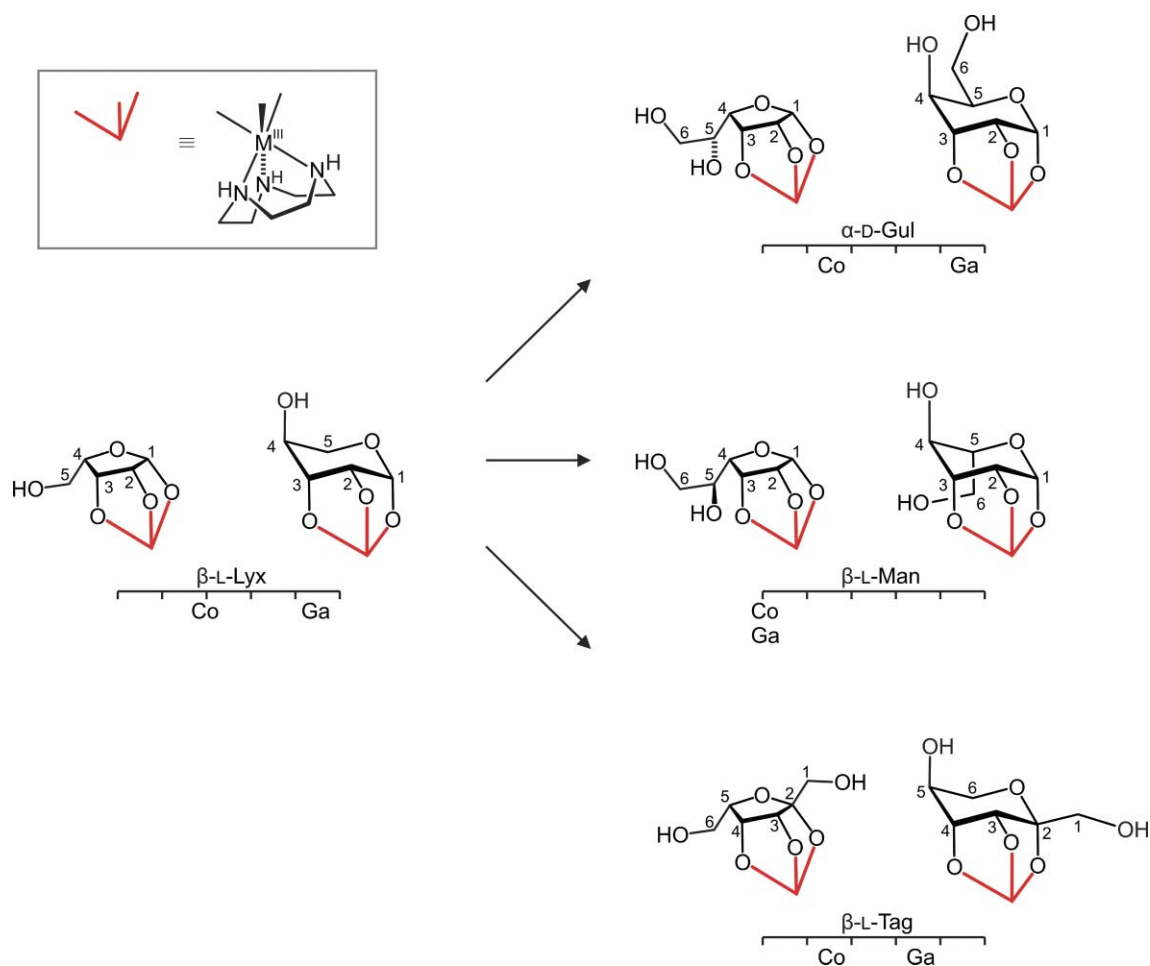
aldopentoses, and eight aldohexoses. In addition, those two of the four ketohexoses are included in the schemes which comply with the *cis-cis* criterion (the rare ketopentose ribulose which complies as well, was not investigated in this study). When the focus is laid on the abundance of the two competing tridentate patterns, it is most fruitful to compare a ribose group (Scheme 2) and a lyxose group (Scheme 3).

The ribose group of tridentate chelators

The ribose group is characterised by a tridentate furanose chelator that has its dangling hydroxymethyl function opposite to the chelating side of the furanose ring. In contrast, the 4-hydroxy function of the pyranose isomer shares the same hemisphere with the O_3 chelator (Scheme 2). In order to illustrate a glycoses' ligand-library properties from an experimental viewpoint, the prototypical case of ribose and one of its homologues, talose, is depicted in Fig. 1. Free ribose, in its aqueous solution equilibrium, is a mixture of four isomers in terms of standard ^{13}C NMR spectroscopy (Fig. 1, top). After reaction with the $\text{Co}^{\text{III}}(\text{tacn})$ probe, only five of the twenty signals remain, more or less shifted downfield (Fig. 1, centre). Species assignment using the methods given in the Experimental revealed the α -D-ribofuranose- $\kappa O^{1,2,3}$ chelator. In agreement with the same deprotonating conditions



Scheme 2 The α -D-ribose group of tridentate glycoses ligands. The scales show the relative amount of furanose and pyranose isomer as estimated from ^{13}C NMR spectra (left limit: 100% furanose, 0% pyranose; right limit: 0% furanose, 100% pyranose) for the $\text{Co}^{\text{III}}(\text{tacn})$ and the $\text{Ga}^{\text{III}}(\text{tacn})$ probe. For the example of α -D-allose (top right), the scale shows 80% allofuranose and 20% allopentopyranose binding to cobalt, whereas the gallium-allofuranose complex is found at 60% quantity leaving 40% for the allopentopyranose chelator.



Scheme 3 The β -L-lyxose group of tridentate glycosyl ligands. The scales show the relative amount of furanose and pyranose isomer (left limit: 100% furanose, 0% pyranose; right limit: 0% furanose, 100% pyranose) for the $\text{Co}^{\text{III}}(\text{tacn})$ and the $\text{Ga}^{\text{III}}(\text{tacn})$ probe ($\text{Ga}^{\text{III}}(\text{Me}_3\text{tacn})$ for lyxose and mannose).

that have been applied in related work on palladium probes (typical pH values are about 11–12 in all cases), ribose trianions are formulated.⁸ It should be noted at this point that in the less complex case of metal bonding by ribofuranose-5-phosphate, which is devoid of pyranose isomers due to its blocked 5-position, the same result was obtained.¹⁴ For the parent glycosyl ribose, however, the result is a particularly instructive example of the dynamic-ligand-library concept since it is the least abundant isomer that gives rise to the optimal ligand, and the three less suitable isomers are transformed into the tridentate α -furanose chelator in the course of the reaction.

Probing the glycosyl chelating sites both with the $\text{Co}^{\text{III}}(\text{tacn})$ and the $\text{Ga}^{\text{III}}(\text{tacn})$ fragment (Tables 1 and 2), the *anti* situation provided by the furanose core clearly led to the more stable metal complexes. When replacing ribose by talose, the prevalence of the furanose as shown in Fig. 1 is maintained, since the talopyranose chelator is markedly destabilised by an axial 6-hydroxymethyl function at the C5 position. The substitution of ribose's H1 by a hydroxymethyl function which leads to psicose, also did not diminish the furanose's prevalence. If, however, the potential pyranose ligand is provided with an equatorial 6-hydroxymethyl function, this form gains some stability, particularly with the gallium probe. Thus, for allose, about 60% of the glycosyl is found as a furanose and about 40% as a pyranose chelator. As

an interim result, the *anti* position of functional groups outside the metal-binding O_3 set appears to be beneficial to a species's stability.

The lyxose group of tridentate chelators

The steric characteristics of lyxose and its homologues are opposite to those of their ribose-group counterparts. It is now the furanose that exhibits a *syn*-5-hydroxymethyl function at C4 whereas lyxopyranose bears an *anti*-4-hydroxy group with respect to the O_3 set. As a result, the α -D-erythrofuranose pattern keeps its overall dominance for the cobalt probe but the pyranose chelator gains stability for the gallium probe, as long as strongly destabilising factors are absent.

Fig. 2 shows an instructive example from the lyxose group. Free lyxose, in its aqueous equilibrium, is dominated by the two pyranose anomers. α -D-Lyxofuranose is a minor component and β -D-lyxofuranose is observed as a trace close to the detection limit of standard NMR techniques. The addition of the cobalt probe, again shows the dynamic ligand-library behaviour of the pentose solution. The major α -D-lyxopyranose isomer vanishes, the β -D-lyxopyranose isomer remains the second most abundant species, and, most remarkably, the overall minor form, the β -D-furanose, is enriched to become the major chelator. If the next step, expanding

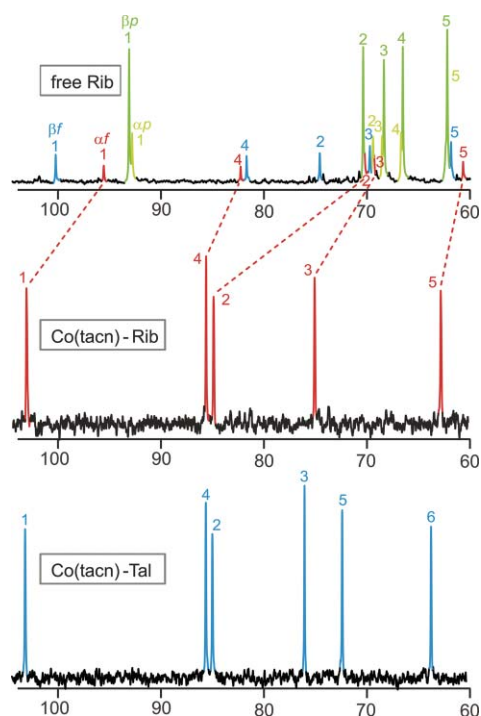


Fig. 1 ^{13}C NMR spectra; dashed lines connect the signals of the free and the bonded pentose. Top: an aqueous solution of D-ribose showing the furanose (red and blue signals denote αf and βf) and pyranose anomeric pairs (lighter and darker green signals denote αp and βp) in their aqueous equilibrium (the numerals refer to standard carbohydrate numbering as used in Scheme 2).²⁰ Centre: the $\text{Co}^{\text{III}}(\text{tacn})$ probe enriches α -D-ribofuranose as the only ligand. Bottom: also D-talose, an aldohexose member of the ribose group, enriches exclusively β -D-talofuranose as a ligand to the $\text{Co}^{\text{III}}(\text{tacn})$ fragment.

lyxose to its aldohexose homologue mannose, is taken, the result is sensible in terms of the two chelating lyxose species. The expansion of the lyxofuranose to mannofuranose leaves a sterically suitable ligand, whereas the tentative mannopyranose chelator is burdened by an unsuitable axial 6-hydroxymethyl function (Scheme 3, centre right). In agreement with the pyranose's destabilisation, Fig. 2 shows the mannofuranose chelator as the only species – which, again, is the least abundant of the four cyclic isomers of the parent aldose.²¹

The introduction of the β -D-mannofuranose chelator marks a good point to address two issues. The first is the contribution of single-crystal analysis, the second is the competition of tridentate chelation and higher-density O_n patterns. To confirm the triple deprotonation of the chelating triol moiety, X-ray analysis would be desirable. Unfortunately, all attempts to crystallise one of the complexes identified above failed, even in the cases where only a single solution species was enriched. However, a proof of the supposed degree of deprotonation, as well as a first impression of the metrical properties of a tridentate glycofuranose chelator, was gained from experiments devoted to homoleptic chromium(III) chelation by glycoses. Under various reaction conditions, mononuclear bis(mannofuranosato)chromates(III) were crystallised that show their furanose ligand bonded the same way as was derived from NMR experiments on the tacn-based probes. The investigation of solution equilibria is preliminary but the results of the structure determination on the homoleptic

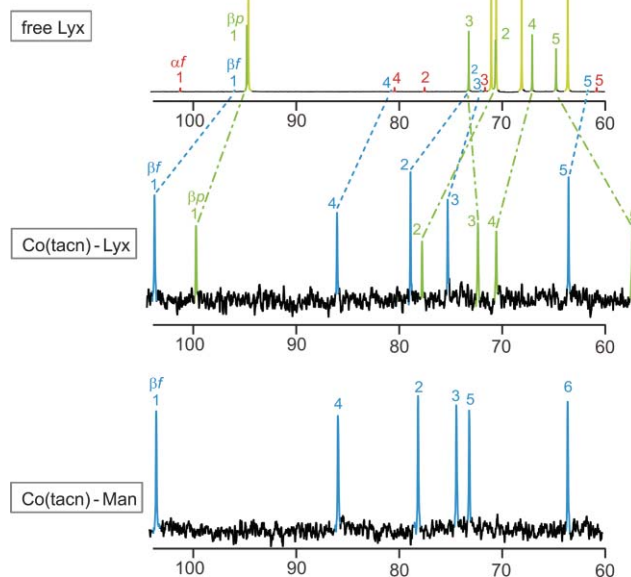


Fig. 2 ^{13}C NMR spectra; dashed lines connect the signals of the free and the bonded pentose. Top: an aqueous solution of D-lyxose showing small amounts of the furanose anomers and the major pyranose anomeric pair in their aqueous equilibrium (the same notation as in Fig. 1 is used).²⁰ Centre: the $\text{Co}^{\text{III}}(\text{tacn})$ probe enriches β -D-lyxofuranose to about two thirds and the β -D-lyxopyranose ligand to about a third. Bottom: D-mannose, an aldohexose member of the lyxose group, enriches exclusively β -D-mannofuranose as a ligand to the $\text{Co}^{\text{III}}(\text{tacn})$ fragment due to a destabilising factor in pyranose chelation.

chromate anion in crystals of the sodium salt supports the conclusions drawn for the tacn compounds of this work. Fig. 3 shows the structure of the anion in green crystals of $\text{Na}_4[\text{Cr}(\beta\text{-D-Man}/1,2,3\text{H}_3)_2]\text{NO}_3 \cdot 8.5\text{H}_2\text{O}$. The trianion's non-crystallographic symmetry is close to C_2 . The E_{C_2} conformation of the furanose rings is close to the results of the coupling-constant analysis on the tridentate furanose ligands in the tacn-type complexes. Accordingly, other structural features such as the intramolecular hydrogen bond of the type $\text{O}5\text{-H} \cdots \text{O}3$ may be typical for the furanose ligands of the lyxose group.

With respect to the second issue, the competition of various oxygen-atom patterns, some facts can be viewed as an interim result of an ongoing investigation. Thus, the glycoses of the *syn* type, as found in the ribopyranose and the lyxofuranose groups, may provide spatially compact O_n atom patterns that exceed tridenticity and thus support edge-, vertex- and face-sharing coordination polyhedra of bi- to polynuclear complexes. Examples include the above-mentioned tetradentate lyxofuranose ligand in a face-sharing dimolybdate, and a couple of homoleptic dimetallates(III) with pentadentate β -mannofuranose pentaanions of the general formula $[\text{M}^{\text{III}}_2(\beta\text{-D-Man}/\text{H}_3)_2]^+$. M is any of the trivalent metal ions of V, Cr, Mn, Fe, Al, and Ga.¹¹ The pentadentate mannose pentaanions, pairs of which provide $(\text{O}_5)_2$ patterns of oxygen atoms, support edge-shared double-octahedra.^{11,22} (A closely related dicobaltate(III) with xylitolato ligands has been

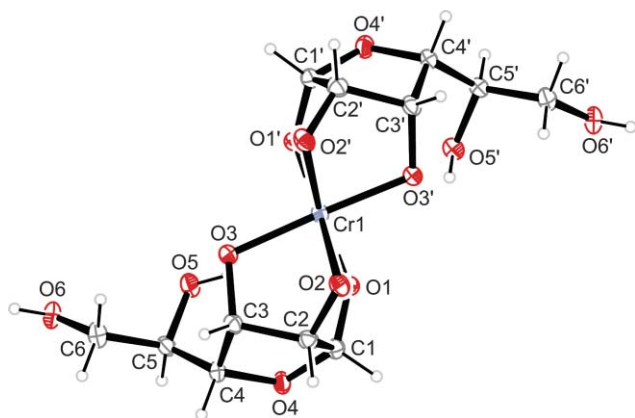


Fig. 3 Structure of the anions in crystals of $\text{Na}_4[\text{Cr}(\beta\text{-D-Manf}/1,2,3\text{H}_3)_2]\text{NO}_3 \cdot 8.5\text{H}_2\text{O}$ (50% probability ellipsoids), projected along the non-crystallographical C_2 axis. Distances (Å) and angles ($^\circ$): from Cr1 to: O2 1.9722(2), O2' 1.9806(2), O3' 1.9833(2), O3 1.9943(2), O1' 1.9994(2), O1 2.0180(2); donor-acceptor distances in intramolecular hydrogen bonds: O5'...O3 2.629(2), O5'...O3' 2.588(2); furanose pucker: $Q_2 = 0.407(2)$, $\varphi_2 = 257.6(3)$ for the ring O4-C1-..., $Q_2 = 0.413(2)$, $\varphi_2 = 259.0(3)$ for the ring O4'-C1'-..., both conformations are close to E_{C2} .

reported as well.²³) At the present stage of investigation, there are two islands of stability for mannose-containing species in the quaternary systems $\text{M}^{\text{III}}/\text{tacn}/\text{D-Man}/\text{OH}^-$: the tacn compounds of this work and the homoleptic dimetallates. It should be noted that the homoleptic monochromate described above seems to be a less stable species that vanishes from the solutions in the course of some weeks in favour of the homoleptic dichromate. Although this part of our investigation is not finished, we can state that the decisive parameter which determines, for mannose, the sole formation of either a tacn-type complex or a homoleptic dimetallate is obvious. It is the stoichiometry including the acid-base balance. Thus, solutions containing equimolar amounts of metal(III) salt and mannose always contained the $[\text{M}^{\text{III}}(\text{tacn})(\beta\text{-D-Manf}/1,2,3\text{H}_3)]$ complex as the major species after the addition of an equimolar amount of tacn and a triple molar amount of hydroxide, whereas addition of five moles of hydroxide in the absence of tacn always yielded the homoleptic dimetallate.

While mannose remains a pure furanose-based tridentate ligand due to the pyranose form's instability, the opposite holds for gulose. Gulopyranose, which exhibits a double *anti* situation for the non-chelating functions, is enriched to about a third part of the total glucose content in the cobalt-containing reaction mixtures and to about 90% of the pyranose ligand with gallium (Scheme 3). The parent glucose, lyxose, parallels the gulose result and thus shows a switch from pure ribofuranose to almost exclusive lyxopyranose chelation for the gallium probe. The ketohexose tagatose, at least, underlines the result obtained with the ribose/psicose pair; that an additional hydroxymethyl function instead of H1 does not markedly alter the chelating properties of the parent aldopentose. A peculiarity of the ^{13}C NMR results is notable. In agreement with the close structural similarities within a group, the chemical shifts of the homologous species match. However, the CIS values show an unexpectedly large deviation in particular for the gallium complexes of the lyxo/gulo-pyranose couple (Tables 3 and 4). The reason seems to be the disparity between the standard and the bonded state. Thus, the $\alpha\text{-D-gulopyranose}$ chelator of Scheme 3

has the same 4C_1 conformation as free $\alpha\text{-D-gulopyranose}$, whereas the ${}^4C_1\text{-}\beta\text{-L-lyxose}$ chelator is expected to switch to 1C_4 on release of the metal. Hence, no reliable CIS values can be given due to the lack of data on the free glucose in its metal-binding conformation.

Since CIS-based confirmation of the assignments made was not obtainable for the $\beta\text{-lyxopyranose}$ ligand in its ${}^1C_4\text{-D}$ or ${}^4C_1\text{-L}$ conformation, a DFT-based prediction of the chemical shifts of the metallated glycoses was used as a substitute. This approach had been validated by means of palladium(II)-glucose complexes whose shifts were calculated with a maximum deviation of approximately 3 ppm by the procedure given in the Experimental (for details, see ESI†). The results of the calculations confirmed the assignments made (Tables 3 and 4). As an example for the pyranose's somewhat "expanded" conformation, the minimum structure of the calculated $\text{Ga}^{\text{III}}(\text{tacn})(\beta\text{-L-Lyxp}/1,2,3\text{H}_3\text{-}\kappa\text{O}^{1,2,3})$ complex is shown in Fig. 4. It should be noted, however, that the calculations did not contribute to the question of why the slightly larger gallium central atoms prefer the pyranose ligand whereas the cobalt centres show a preference for the furanose chelator. In terms of energies in the gas phase, the furanose is always more stable. Hence, the stability relationships obviously depend on the variably efficient incorporation of the complexes in a hydrogen-bonded environment.

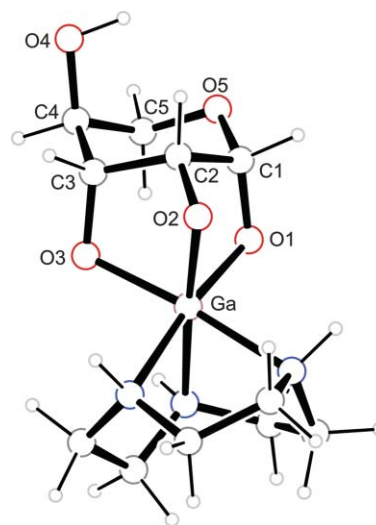
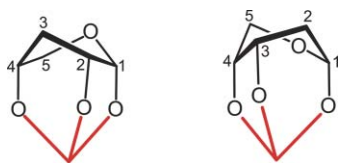


Fig. 4 The molecular structure of $\text{Ga}^{\text{III}}(\text{tacn})(\beta\text{-L-Lyxp}/1,2,3\text{H}_3\text{-}\kappa\text{O}^{1,2,3})$ as calculated on the BLYP/CEP-4G/6-31+G(2d,p) level of theory. Distances (Å) from Ga to: O1 1.948, O2 1.929, O3 1.923, N_{mean} 2.248. Calculated values for the homologous cobalt complex: from Co to: O1 1.917, O2 1.891, O3 1.905, N_{mean} 2.014.

Epimerisation of threose homologues

The conceptual restriction of considering only one half of all the glycoses as potential tridentate chelators stems from the exclusion of the non-chair conformations of the potential pyranose ligands. It should be noted, however, that the full number of glycoses can be considered tridentate chelators if some not-too-unstable conformers such as skew-boats are permitted as ligands. Examples are given in Scheme 4 for two parent patterns that can be completed to depict arabinose and xylose and so open a way to the missing threose branch.



Scheme 4 Two skew-boat conformers that may be suggested as tridentate chelators. Left: the $^{3.0}B$ conformation of 3-deoxy-D-erythro-pentopyranose which branches to D-ribose and D-xylose on addition of a 3-hydroxy function. Right: the $^{2.5}B$ conformation of 2-deoxy-D-erythro-pentopyranose (the pyranose form of “2-deoxy-D-ribose”) which branches to D-ribose and D-arabinose on addition of a 2-hydroxy function.

Although glucose boat conformers have been found in the active sites of metalloenzymes, however, the reaction conditions applied in this work open an alternative to the glycoside.²⁴ In agreement with the non-neutral pH range and the presence of a strongly chelating metal centre, base-catalysed 2-epimerisation takes place forming the corresponding isomer of the well-suited half of the glycosides. The reaction was most straightforward for arabinose which, under the standard reaction conditions, yielded the same spectra of the pure ribofuranose chelator with the cobalt probe as did ribose itself. Other reaction mixtures contained some unidentified products but the cobalt-bonded epimers were usually the major forms and include lyxose from xylose and talose from galactose. The analysis of further, more complex reaction mixtures and some unresolved cases is beyond the scope of this work and will be investigated in the future. We included the reaction of the cobalt probe with fructose which was expected to end with particular ease at mannose, but did not.

It should be noted that epimerisation towards the ligand of required hapticity is a well-established phenomenon in carbohydrate chemistry. The direction of epimerisation is particularly clear when, as is the case here also, the denticity and the bonding mode of the ligand is known. Thus, a similar reaction of xylose to lyxose was described almost three decades ago in the course of binding a binuclear dimolybdate unit to a tetradentate ligand which is not provided by any D-xylose isomer but by the β -furanose isomer of the 2-epimer D-lyxose.^{9,10}

Erythrose

One would expect that erythrose provides the prototypical α -D-erythro-furanose chelator in a particularly distinct way. However, as has been demonstrated for the bidentate metal-binding mode, erythrose is special.⁸ The rules that emerge from the investigation of pentoses and hexoses imply the instability of open-chain isomers which, conversely, are not enriched from the ligand library by rather “unobtrusive” probes such as gallium and cobalt. Open-chain erythrose isomers, particularly the aldehyde hydrate, are present in a considerable quantity and have decisive influence on the erythrose’s reactivity. Hence, with the gallium probe, we were unable to interpret the signal-rich spectra. With the cobalt probe, however, about two thirds of the glycoside was found in the expected bonding mode (Table 1). Strongly down-field-shifted signals of the aldehyde/carboxylate region were present as well but were not assigned.

Conclusions

In conclusion, tridentate glycoside libraries are markedly restricted in comparison to bidentate libraries. Using the $M^{III}(\text{tacn})$ probes with cobalt and gallium, only two basic chelators were observed, the α -D-erythro-furanose- $\kappa O^{1,2,3}$ and the 4-deoxy- α -D-erythro-pentopyranose- $\kappa O^{1,2,3}$ pattern (Scheme 1). Of these, the furanose chelator is the more abundant. For an individual glycoside, a pattern gains significance if the remaining substituents are in an *anti* position to the O_3 moiety. In addition, an aldohexose’s 6-hydroxymethyl function is influential. In an equatorial position, this function stabilises the pyranose, whereas an axial 6-hydroxymethyl function definitely prevents pyranose chelation. Applying these rules to the common aldoses and ketoses, tridentate furanose chelation dominates the glycosides with the ribose partial structure, namely, ribose, allose, talose, and psicose. Only in the case of allose does the 6-hydroxymethyl criterion stabilise the pyranose chelator to some extent. In contrast, pyranose chelation gains significance for the glycosides with the lyxose partial structure: lyxose, gulose, and tagatose. The 6-hydroxymethyl criterion excludes mannose from this group. For those glycosides that do not possess the essential *cis,cis-O*^{1,2,3} pattern, the chosen experimental boundary conditions allow 2-epimerisation to a suitable tridentate chelator. Due to this alternative, our experimental set-up leaves no chance for pyranose conformations other than the stable chair. Conversely, in order to check whether or not a central metal accepts tridentate glycoside chelation, a trial with ribose and lyxose should suffice.

A methodological caveat, however, has to be observed in any screening for glycoside chelation. Thus, the use of coordination-induced shifts (CISs) in the paradigmatic way, where a CIS shows the metal-binding site and, conversely, where the absence of a CIS detects a non-metallated function, is misleading. CIS-based argumentation fails if the reference state cannot be properly chosen. Thus, the ¹³C NMR spectrum of chair-inverted ¹C₄- β -D-lyxopyranose, whose chemical shifts appear to be substantially different from those of the ⁴C₁ conformer, is unknown. CIS values that are calculated as the difference between the signal positions of the chelating ¹C₄ and the free ⁴C₁ form, are thus meaningless. As a powerful tool to resolve this situation, DFT-based chemical shifts and coupling constants should be correlated with the experimental values.

Keeping in mind the peculiarities of glycoside chelation, coordination chemists will, hopefully, take advantage of these most abundant biomolecules’ ability to incorporate a metal of sufficient Lewis acidity in a thermodynamically stable chelate.

Acknowledgements

The authors thank Sandra Albrecht for technical assistance, and Thorsten Allscher for the lyxose NMR spectrum.

References

- 1 W. Plass, *Coord. Chem. Rev.*, 2009, **253**, 2286–2295.
- 2 M. Gottschaldt and Ulrich S. Schubert, *Chem.–Eur. J.*, 2009, **15**, 1548–1557.
- 3 C. G. Hartinger, A. A. Nazarov, S. M. Ashraf, P. J. Dyson and B. K. Keppler, *Curr. Med. Chem.*, 2008, **15**, 2574–2591.

- 4 G. Erre, S. Enthaler, K. Junge, S. Gladiali and M. Beller, *Coord. Chem. Rev.*, 2008, **252**, 471–491.
- 5 M. Diéguez, C. Claver and O. Pàmies, *Eur. J. Org. Chem.*, 2007, 4621–4634.
- 6 V. Benessere, R. Del Litto, A. De Roma and F. Ruffo, *Coord. Chem. Rev.*, 2010, **254**, 390–401.
- 7 T. Storr, Y. Sugai, C. A. Barta, Y. Mikata, M. J. Adam, S. Yano and C. Orvig, *Inorg. Chem.*, 2005, **44**, 2698–2705.
- 8 Y. Arendt, O. Labisch and P. Klüfers, *Carbohydr. Res.*, 2009, **344**, 1213–1224.
- 9 G. E. Taylor and J. M. Waters, *Tetrahedron Lett.*, 1981, **22**, 1277–1278.
- 10 T. Allscher and P. Klüfers, *Carbohydr. Res.*, 2009, **344**, 539–540.
- 11 J. Burger, C. Gack and P. Klüfers, *Angew. Chem., Int. Ed.*, 1995, **34**, 2647–2649.
- 12 A. S. Perlin, *Methods in carbohydrate chemistry*, Wiley, New York, NY [a.o.], 1962.
- 13 H. E. Gottlieb, V. Kotlyar and A. Nudelman, *J. Org. Chem.*, 1997, **62**, 7512–7515.
- 14 K. Gilg, T. Mayer, N. Ghaschgaie and P. Klüfers, *Dalton Trans.*, 2009, 7934–7945.
- 15 C. A. G. Haasnoot, F. A. A. M. de Leeuw and C. Altona, *Tetrahedron*, 1980, **36**, 2783–2792.
- 16 M. J. Frisch, G. W. Trucks, H. B. Schlegel, G. E. Scuseria, M. A. Robb, J. R. Cheeseman, J. A. Montgomery, Jr., T. Vreven, K. N. Kudin, J. C. Burant, J. M. Millam, S. S. Iyengar, J. Tomasi, V. Barone, B. Mennucci, M. Cossi, G. Scalmani, N. Rega, G. A. Petersson, H. Nakatsuji, M. Hada, M. Ehara, K. Toyota, R. Fukuda, J. Hasegawa, M. Ishida, T. Nakajima, Y. Honda, O. Kitao, H. Nakai, M. Klene, X. Li, J. E. Knox, H. P. Hratchian, J. B. Cross, V. Bakken, C. Adamo, J. Jaramillo, R. Gomperts, R. E. Stratmann, O. Yazyev, A. J. Austin, R. Cammi, C. Pomelli, J. Ochterski, P. Y. Ayala, K. Morokuma, G. A. Voth, P. Salvador, J. J. Dannenberg, V. G. Zakrzewski, S. Dapprich, A. D. Daniels, M. C. Strain, O. Farkas, D. K. Malick, A. D. Rabuck, K. Raghavachari, J. B. Foresman, J. V. Ortiz, Q. Cui, A. G. Baboul, S. Clifford, J. Cioslowski, B. B. Stefanov, G. Liu, A. Liashenko, P. Piskorz, I. Komaromi, R. L. Martin, D. J. Fox, T. Keith, M. A. Al-Laham, C. Y. Peng, A. Nanayakkara, M. Challacombe, P. M. W. Gill, B. G. Johnson, W. Chen, M. W. Wong, C. Gonzalez and J. A. Pople, *GAUSSIAN 03 (Revision D.01)*, Gaussian, Inc., Wallingford, CT, 2004.
- 17 W. J. Stevens, M. Krauss, H. Basch and P. G. Jasien, *Can. J. Chem.*, 1992, **70**, 612–630.
- 18 A. Altomare, M. C. Burla, M. Camalli, G. L. Cascarano, C. Giacovazzo, A. Guagliardi, A. G. G. Moliterni, G. Polidori and R. Spagna, *J. Appl. Crystallogr.*, 1999, **32**, 115–119.
- 19 G. Sheldrick, *Acta Crystallogr., Sect. A: Found. Crystallogr.*, 2008, **64**, 112–122.
- 20 K. N. Drew, J. Zajicek, G. Bondo, B. Bose and A. S. Serianni, *Carbohydr. Res.*, 1998, **307**, 199–209.
- 21 Y. Zhu, J. Zajicek and A. S. Serianni, *J. Org. Chem.*, 2001, **66**, 6244–6251.
- 22 J. Burger and P. Klüfers, *Z. Anorg. Allg. Chem.*, 1997, **623**, 1547–1554.
- 23 J. Burger and P. Klüfers, *Z. Anorg. Allg. Chem.*, 1998, **624**, 359–360.
- 24 W. Zhong, D. A. Kuntz, B. Ember, H. Singh, K. W. Moremen, D. R. Rose and G.-J. Boons, *J. Am. Chem. Soc.*, 2008, **130**, 8975–8983.